ORIGINAL ARTICLE

XYLEM INTERMIXED WITH PHLOEM1, a leucine-rich repeat receptor-like kinase required for stem growth and vascular development in *Arabidopsis thaliana*

**Anthony C. Bryan · Adam Obaidi ·
Michael Wierzba · Frans E. Tax**

Abstract The regulation of cell specification in plants is particularly important in vascular development. The vascular system is comprised two differentiated tissue types, the xylem and phloem, which form conductive elements for the transport of water, nutrients and signaling molecules. A meristematic layer, the procambium, is located between these two differentiated cell types and divides to initiate vascular growth. We report the identification of a receptor-like kinase (RLK) that is expressed in the vasculature. Histochemical analyses of mutants in this kinase display an aberrant accumulation of highly lignified cells, typical of xylem or fiber cells, within the phloem. In addition, phloem cells are sometimes located adjacent to xylem cells in these mutants. We, therefore, named this RLK XYLEM INTERMIXED WITH PHLOEM 1 (XIP1). Analyses of longitudinal profiles of *xip1* mutant stems show malformed cell files, indicating defects in oriented cell divisions or cell morphology. We propose that XIP1 prevents ectopic lignification in phloem cells and is necessary to maintain the organization of cell files or cell morphology in conductive elements.

Keywords LRR RLKs · Phloem · Procambium · Vasculature · Xylem

A. C. Bryan · A. Obaidi · M. Wierzba · F. E. Tax
Department of Molecular and Cellular Biology,
University of Arizona, Tucson, AZ 85721, USA

F. E. Tax (✉)
Department of Plant Sciences, University of Arizona,
Tucson, AZ 85721, USA
e-mail: fetax@email.arizona.edu

Abbreviations

XIP1	XYLEM INTERMIXED WITH PHLOEM 1
RLK	Receptor like kinase
LRR	Leucine rich repeat
SAM	Shoot apical meristem
RAM	Root apical meristem
TB	Toluidine blue

Introduction

To coordinate growth within plant organs, the developmental identities of cells must be specified and maintained. Synchronous growth is especially important for the development of the plant vascular system, where adjoining cells in single longitudinal files share the same cellular identity and form conductive elements that transport various substances throughout the plant body (Ye 2002). Plant structural support and the transport of water, nutrients, and signaling molecules are dependent on the specialized cells of the xylem and phloem. Although these vascular tissues are vital to plant survival, the mechanisms for the specification and maintenance of their identities remain largely unknown.

In adult plants, the majority of cells arise from stem cell populations found in the shoot apical meristem (SAM) and in the root apical meristem (RAM). Although the SAM and RAM stem cell niches are organized differently, both utilize a conserved intercellular signaling mechanism comprised a secreted peptide, a receptor-like kinase (RLK), and a homeobox transcription factor to maintain stem cells (Stahl and Simon 2010). The xylem and phloem arise from a vascular meristem located between them known as the

procambium. Procambium function is characterized by oriented cell divisions which generate xylem to the center of the organ and phloem to the periphery (Scheres et al. 1995; Galweiler et al. 1998). The initial meristematic cells that contribute to vascular tissues are formed during early embryogenesis, at the globular stage (Scheres et al. 1995). Although vascular cells are present in late embryogenesis, they do not fully differentiate until after germination.

The cambium is a secondary meristem that is derived from the procambium in the adult plant and is responsible for secondary growth in the diameter of stems and roots through the production of phloem and xylem. The cambium also regulates the lateral growth of the interfascicular region, the connective tissue between vascular bundles in the stem. In Arabidopsis, the development of the cambium is confined to the base of the stem, the hypocotyl and the mature root (Altamura et al. 2001), although how cambium formation is regulated is not known. Cambium activity, however, has been shown to be increased in plants over-expressing *Arabidopsis thaliana* HOMEOBOX GENE 8 (*At*HB8), an HD ZIP transcription factor involved in procambium initiation and cell proliferation (Baima et al. 2001; Kang and Dengler 2002; Donner et al. 2009). These plants showed increased proliferation and differentiation of xylem cells and ectopic lignification of phloem and pith cells. In addition, *high cambium activity* (*hca*) mutants were identified that have altered vascular bundle organization and increased expression of *At*HB8 (Pineau et al. 2005). Mutations in two RLKs, REDUCED IN LATERAL GROWTH1 (RUL1) and MORE LATERAL GROWTH1 (MOL1), resulted in a reduced interfascicular region and an expanded interfascicular region, respectively, suggesting a role of intercellular signaling in regulating cambium activity (Agusti et al. 2011). The precise onset of the initiation of cambium formation during development is not completely understood, nor is it understood how the cambial meristem contributes to regulating the specification of the secondary xylem and phloem cells, nor how the procambium contributes to maintaining vascular cell identity. In general, when compared to the SAM and RAM, much less is known about how the procambial and cambial meristems are specified and maintained.

Although several genes have been identified that regulate the initiation and maintenance of the vascular cells, fewer genes have thus far been associated with the specification of distinct cell types. Two NAC domain transcription factors, VASCULAR-RELATED NAC DOMAIN 6 and 7 (VND6 and VND7), promote the differentiation of various cell types including non-vascular tissues such as leaf epidermis and mesophyll and root cortex into metaxylem (mature xylem) and protoxylem (initial xylem) when overexpressed, respectively (Kubo et al. 2005). The only gene known to be required for determining phloem cell identity

is ALTERED PHLOEM DEVELOPMENT (APL), a MYB coiled-coil transcription factor. APL is necessary for the specification of phloem companion cells and sieve elements and limits the differentiation of xylem cells (Bonke et al. 2003). However, the mechanisms that regulate APL are not yet known.

A signaling mechanism has recently been described to regulate procambium activity by controlling cell proliferation and xylem differentiation. The Leucine Rich Repeat (LRR) RLK PHLOEM INTERCALATED WITH XYLEM (PXY), which is expressed mainly in the procambium, controls the oriented cell divisions of the procambium (Fisher and Turner 2007). In *pxy* mutants, phloem cells are found adjacent to and intermixed with xylem cells in inflorescence stems. PXY is a receptor for the tracheary element differentiation factor (TDIF) peptide, a small secreted peptide originating from the phloem and encoded by the CLAVATA3/ESR 41/44 (CLE41/44) genes. Exogenous application of CLE41/44 peptide to seedlings inhibits formation of xylem vessels in leaves and increases the number of procambium cells in hypotcotyls; *pxy* mutants are insensitive to the effects of CLE treatment (Hirakawa et al. 2008). Additionally, CLE41/44 has been shown to activate WUSCHEL RELATED HOMEOBOX 4 (WOX4) in a PXY-dependent manner (Hirakawa et al. 2010). However, WOX4 regulates procambium proliferation, and not xylem cell differentiation. Thus, a current model suggests CLE41/44 is secreted from phloem cells and binds PXY in the procambium, activating the WOX4 signaling pathway to regulate cell division in the procambium. This mechanism is similar to the CLV3-CLV1-WUS signaling mechanism controlling stem cells in the SAM and CLE40-ACR4-WOX5 signaling in the RAM (Clark et al. 1993; Clark et al. 1997; Schoof et al. 2000; Brand et al. 2002; Sarkar et al. 2007; Stahl et al. 2009). However, CLE41/44 peptide is a positive regulator of stem cell proliferation in procambium tissue, rather than acting by repressing as CLV3 does in the SAM.

In this study, we identified an LRR RLK that is expressed in the vasculature and, we hypothesize, functions in vascular development. We demonstrate that mutants in this RLK lead to accumulation of cells with ectopic lignification in regions of phloem in the vascular bundles of inflorescence stems. However, mutant alleles in this RLK also lead to phloem cells adjacent to xylem cells, similar to *pxy* mutants, suggesting it additionally influences organization of tissue identities in vascular bundles. We, therefore, named this RLK XYLEM INTERMIXED WITH PHLOEM 1 (XIP1). Mutant phenotypes suggest XIP1 plays a role in differentiation of phloem cells in vascular development. These phenotypes are mainly apparent at the base of the stem, suggesting the defects could be influenced by the effects of secondary growth regulated by cambium

activity. XIP1 is also necessary for the organization or the morphological development of conductive elements in the vasculature.

Materials and methods

Growth conditions and genetic analyses

The *xip1-1* allele was generated by the Seattle TILLING Project (Till et al. 2003). The *xip1-2* allele was obtained from the RIKEN transposon collection (RATM11-2459-1 H). The *xip1-1* allele was back-crossed seven times into the Col-0 ecotype. All lines were grown at 22°C in a Conviron growth chamber with a 16 h light/8 h dark cycle. To genotype the *xip1-1* allele, two primer polymerase chain reaction was performed using NEB Taq and the PCR product was subsequently digested with *Hpa*II (Fermentas), as the *xip1-1* mutation disrupts an *Hpa*II restriction site. The *xip1-2* allele was genotyped using three primer polymerase chain reaction using Ex-Taq (TaKaRa). Primers used for *xip1-1*: *xip1-1* F 5′CTCTCTGGTCCTATCCC CGTCTCAT, *xip1-1* R 5′ACGTCGCATTTGATCGTTGC TTTGG, and PCR for *xip1-2*: *xip1-2* F 5′TCAGAGCTGT TTATGCAGAGTAACA, *XIP1*-2 R 5′GATGATCTGAA TTGGGAGAATTAAA and DS5-1 5′GAAACGGTCG GGAAACTAGCTCTAC. RNA for RT-PCR was extracted from 100 mg of whole seedlings, 6 days after germination, using RNEasy Extraction Kit (Qiagen). 1 μg of total RNA was used for first strand synthesis using gene-specific primers. Primers used for RT-PCR of XIP1CT: XIP1 CT RT F 5′AAATCGACAAACATCTTGTTGGATG, XIP1 CT RT R 5′TAATCTTGGTCGTAGGTTTGGAGGT; XIP1 NT: XIP1 NT F 5′TCAGAGCTGTTTATGCAGAG TAACA, XIP1 NT R 5′AAGAGATTCAAGAATC TCCCTTTGGTCG, and ACT7: ACT7 F 5′-GGTGA GG ATATTCAGCCACTTGTCTG, ACT7 R 5′TGTGAGATC CCGACCCGCAA GATC.

XIP1 promoter and translational fusions

The XIP1 promoter construct was generated by amplifying the 2.5 kb region upstream of the XIP1 start codon (Primers: XIP1 PF F 5′TCGTCAGAGAGTGTCATAA TAGCA, XIP1 PF R 5′TTCAGAGAAAGATCAAAAGT AACCTAG) and cloning it into pCR8-TOPO using the TOPO cloning kit (Invitrogen). Using the LR Gateway system (Invitrogen), the XIP1 promoter was subcloned into pBIB-GUS-BASTA vector (Gou et al. 2010). The XIP1 translational fusion was generated by amplifying the 2.5 kb upstream region from the XIP1 start codon in addition to the genomic sequence minus the stop codon (Primers: XIP1 TF F 5′GCAGGCGGCAAATTACTTTTAATT, XIP1 TF

R 5′GAGTCTTGTTTGCGTGAGATGATCT). The amplified product was cloned into pCR8-TOPO and subcloned into the pBIB-GFP-BASTA vector (Gou et al. 2010). The promoter fusion construct was transformed into Col-0 plants and the translational fusion constructs were transformed into Col-0 and *xip1-1* via *Agrobacterium*-mediated transformation (Clough and Bent 1998).

To analyze lines carrying the XIP1 promoter fusion construct, tissue samples were cut and fixed in 90% acetone and stained with GUS staining solution containing X-Gluc [1 mM X-Gluc (Gold Bio Technology) dissolved in DMSO, 10 mM EDTA, 2 mM potassium ferrocyanide, 0.5 mM potassium ferricyanide, 0.5 mM potassium ferrocyanide, 0.1% Triton X-100, 100 mM NaH$_2$PO4, pH 7.0] for 2–14 h and mounted in ddH$_2$O. To visualize the radial pattern of expression, hand-cut cross sections were obtained and stained with GUS staining solution for 2–14 h and mounted in ddH$_2$O on glass slides (Fisher and Turner 2007). Images of plant organs were taken using a Canon Power Shot SX110 digital camera mounted on a Leica dissecting microscope. Hand-cut section images were taken using a Zeiss Axioplan microscope and QCapture Pro 5.0 imaging software.

Roots from lines carrying the translational fusion construct were grown on 0.5× MS plates for at least 5 days and mounted in 10% glycerol on microscope slides. Imaging of roots was performed using a Nikon 510 meta-confocal microscope and LSM imaging software.

Microscopy and histochemical analysis

Hand-sections of inflorescence stems were cut using a double edged razor and suspended in ddH$_2$O as described (Lux et al. 2005). Toluidine blue and aniline blue staining procedures were conducted as described by Fisher and Turner (2007). Staining hand-cut sections with Maule reagent and phloroglucinol-HCl were performed as described previously (Guo et al. 2001). All stained sections were visualized using a Zeiss Axioplan microscope and QCapture Pro 5.0 imaging software. Of twenty samples of each of the genotypes stained with toluidine blue, blue staining cells in the phloem were seen in all twenty *xip1* samples for each allele, and no blue cells were found in wild-type controls. Twelve samples for each genotype of phloroglucinol with no staining detected in the phloem for the wild type controls and all samples of *xip1* mutants showing staining in phloem. Twelve samples of each genotype were stained with Maule reagent, with no abnormal staining detected in the phloem of wild-type controls, and all *xip1* mutants showing red staining in phloem. In analine blue stained sections, 4/12 individuals showed phloem cells adjacent to xylem cells in *xip1-2* mutants, and 8/12 *xip1-1* individuals were identified with

phloem cells adjacent to xylem cells. All aniline blue stained *xip1* mutants showed blue staining in the phloem.

Thin plastic sections were obtained using the following protocol. Inflorescence stems were cut and fixed in 2% gluteraldehyde/1× PBS solution for 3–4 h and then subjected to an ethanol dehydration series (30, 50, 70, 90, 100% ×2). The tissues were infiltrated with LR white resin (electron microscopy sciences) and placed in plastic molds. 13 μm thin sections were cut using a Sorvall MT2-B Ultra microtome. Sections were stained with TB as described above and visualized using a Zeiss Axioplan microscope and QCapture Pro 5.0 imaging software. Six samples of each genotype were analyzed.

For propidium iodide staining, whole-mount inflorescence stems of 4-week-old plants were treated as described in Przemeck et al. (1996). Stems were fixed in 6:1 EtOH:acedic acid for 2–4 h. After fixation, samples were rehydrated using a series of 10 min washes (100% EtOH, 70% EtOH, 50% EtOH, 30% EtOH, 10% EtOH, ddH$_2$O) and stained with 5 μg/ml propidium iodide for 2–4 h. Six stems of each genotype were cut longitudinally and mounted in chloralhydrate/glycerol/water (8:1:2). Images were taken using epiflourescence optics and a Zeiss axioplan microscope and QCapture Pro imaging software. Misaligned cells were seen in all mutant stems and not present in wild-type controls. Images were taken from the apical portion of stems. Six samples of each allele were analyzed. All Col-0 and Nos (six individuals each of Col-O and Nos) samples showed continuous xylem elements. All samples of *xip1* mutants showed mis-alignment or discontinuous elements.

For height growth measurements, plants were grown on soil for 3 weeks and individual plants measured from the base to the apex of the main bolt. Samples included 32 Col-0, 33 *xip1-1,* 25 Nos, and 46 *xip1-2*. Standard error was determined and t-tests indicate significance between Col-0 and *xip1-1* $p < 0.001$, and between Nos and *xip1-2* $p = 0.01$.

Results

Mutants in At5g49660, an LRR RLK, affect plant growth and cause anthocyanin accumulation in leaves

In the *Arabidopsis thaliana* genome, over 400 genes have been annotated as RLKs including over 200 LRR RLKs (Shiu and Bleecker 2001). The function of the majority of these RLKs remains unknown. In a reverse genetic screen to determine the roles of unknown RLKs involved in *Arabidopsis* development, we isolated insertion mutant alleles for a large subclass of LRR RLKs and screened for developmental phenotypes. There were no insertion mutant

alleles available for At5g49660, so this gene was investigated further. At5g49660 encodes an LRR RLK with 16 extracellular LRRs flanked by two pairs of cysteine residues, a transmembrane domain and a cytoplasmic kinase domain containing the conserved kinase sub-domains associated with an active kinase (Fig. 1a, S1). Using the amino acid sequence of the kinase domain as determined by pfam (http://pfam.sanger.ac.uk), the phylogenetic relationship of At5g49660 was compared with other closely related LRR RLKs (Shiu and Bleecker 2001) using MAFFT sequence alignment, and a phylogenetic tree was created using PhyML (http://mobyle.pasteur.fr/cgi-bin/portal.py#welcome). The resulting phylogenetic tree confirms At5g49660 is part of the LRR XI family, showing distant similarity to CLAVATA1 (CLV1) (45% amino acid identity) and PXY (49% amino acid identity) (Fig. 2). At5g49660 is most similar to a gene involved in endosperm development, HAIKU2 (IKU2), (Luo et al. 2005), but in a pair-wise comparison, the 48% amino acid identity suggests these two kinase domains have diverged significantly in their functions. Based on the high degree of sequence divergence between At5g49660 and LRR X, XI, and XIII subfamilies of RLKs, there was no hint to the role of At5g49660. To determine the function of At5g49660, we isolated seven ethylmethane sulphonate (EMS) mutated lines (Fig. 1a) using the "Targeting Induced Local Lesions IN Genomes" (TILLING) resource (Till et al. 2003). Once identified, mutants were backcrossed into the Col-0 accession and screened for phenotypic defects. Of the 7 missense mutations in At5g49660 identified through TILLING, all of the mutations are located in the extracellular LRR region except for one mutation, which is a substitution of a serine to a phenylalanine at position 677 (S677P) (Fig. S1) in the kinase domain. The S677P mutation is adjacent to sub-domain 1 in the kinase domain and eliminates a semi-conserved serine residue (Fig. S1). *Arabidopsis* plants homozygous for the S677P mutation in At5g49660 were the only plants identified from the TILLING screen that exhibited an obvious mutant phenotype. In these mutant plants, the inflorescence stems were shorter than the Col-0 accession plants (Fig. 1b, f), although general morphology and fertility were normal. In addition, the cotyledons and rosette leaves of plants with the S677P mutation had a purple color, indicative of anthocyanin accumulation (Fig. 1c).

An insertion mutation in At5g49660 was later identified in the RIKEN collection of *Arabidopsis* DS transposon lines (stock # RATM11-2459-1 H). This insertion mutation is located within the coding region of the kinase domain (at amino acid 769) and therefore should represent a null allele (Fig. 1a). RT-PCR of At5g49660 RNA from seedlings homozygous for the insertion allele does not produce RNA corresponding to the C-terminal region downstream of the
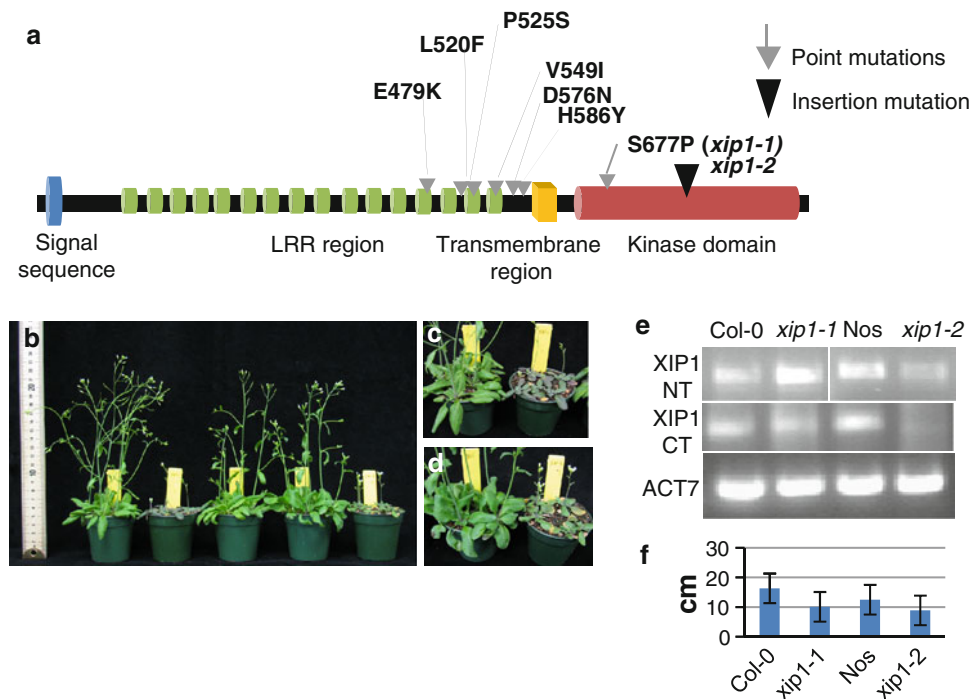
Fig. 1 Gene model of XIP1 and growth defects of *xip1* mutants. **a** Gene model of XIP1 with protein domains and mutant alleles shown. **b** *xip1* mutants show reduced growth compared to wild type plants, from *left* to *right* Col-0, *xip1-1*, *xip1-1* XIP1::GFP, Nos, *xip1-2*. **c, d** Anthocyanin accumulation in *xip1-1* and *xip1-2* plants (*right*) compared to Col-0 and Nos (*left*), respectively. **e** RT-PCR of

XIP1 transcript from RNA samples from seedlings 6 days after germination; from *right* to *left*: Col-0, *xip1-1*, Nos and *xip1-2*. **f** Height of Col-0 and *xip1-1* plants and Nos and *xip1-2* plants measured 4 weeks after germination. *Error bars* represent the standard error, and *t* test analysis shows a significance of $p < 0.001$ between Col-1 and *xip1-1*, and $p < 0.01$ between Nos and *xip1-2*

insertion, but does express RNA from the N-terminal region (Fig. 1e, f). Therefore, plants homozygous for the insertion do not express a full length transcript. Comparison of the growth characteristics of plants homozygous for the insertion in At5g49660 to wild-type Nossen (Nos) accession plants showed similar phenotypes as plants homozygous for the S677P missense mutation, including reduced growth and accumulation of anthocyanin (Fig. 1b, d, f).

In order to show that the S677P mutation in At5g49660 is responsible for the phenotypes observed, we complemented plants homozygous for the S677P mutation with a wild-type copy of the At5g49660 gene. The genomic region of At5g49660 including 2.5 kb upstream of the coding sequence was fused with the sequence for green florescent protein (GFP), creating a C-terminal translational fusion. Plants with the S667P mutation in At5g49660 transformed with this At5g49660:GFP fusion showed similar height compared to wild-type plants and also lacked noticeable anthocyanin accumulation in leaves (Fig. 1b). The ability to rescue the phenotypes associated with the missense mutation with a wild-type copy of the At5g49660 gene provides further evidence that the mutant phenotype is due to the mutation in At5g49660.

At5g49660 is expressed in the vasculature throughout development

Gene expression data can provide clues to determine the cellular basis of growth defects. To determine which cell types At5g49660 is expressed in, we generated a promoter fusion by cloning the putative At5g49660 promoter upstream of the β-glucuronidase (GUS) reporter gene. The 2.5 kb sequence upstream of the start codon, identical to that used in the genomic rescue clone, was fused to the GUS coding sequence. After transformation of Col-0 plants, eight independent lines were analyzed for GUS activity. GUS activity was detected in the vasculature, beginning with the mature embryo stage through the adult plant in all eight lines (Fig. 3). At5g49660 was expressed in the vasculature of stems, leaves, sepals, pedals, pedicels, hypocotyls and roots (Fig. 3b–l). Hand-cut cross sections of stems and pedicels show expression within the phloem and procambium regions of the vasculature (Fig. 3c–e, g, i). Vascular expression of At5g49660 in roots was analyzed using the translational fusion to GFP (Fig. 3l) and microarray expression analyses available in the AREX database (Birnbaum et al. 2003; Brady et al. 2007). Based on the AREX data, At5g49660 is restricted to the phloem and
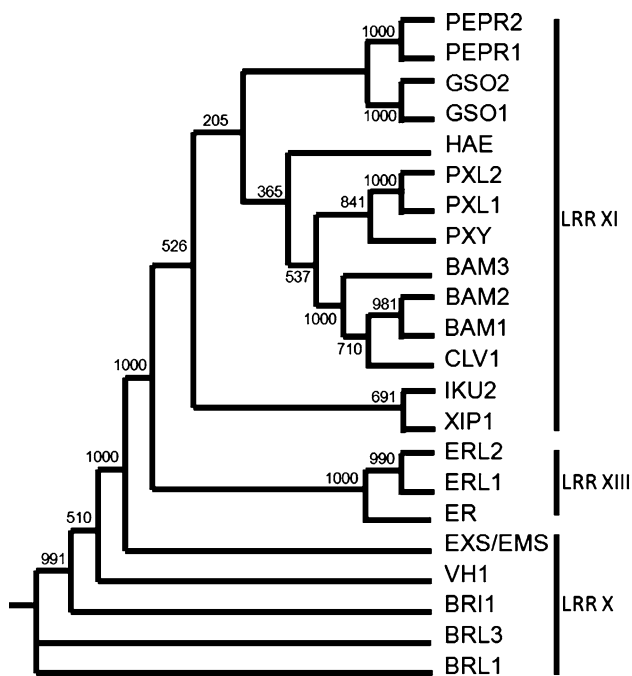
Fig. 2 Phylogenetic analysis of kinase domains related to XIP1 in LRR RLK families X, XI, and XIII. The kinase domain, as determined by pfam database, was used to align the amino acid sequences of a subset of related RLKs. The phylogeny was determined using phylogenies by maximum likelihood analysis with bootstrap values provided. This phylogenetic tree includes RLKs involved in many different processes including responses to stress (PEPR1, PEPR1), abscission (HAE), SAM maintenance (CLV1, BAM1, BAM2, BAM3), endosperm development (IKU2), brassinosteroid perception (BRI1, BRL1, BRL3), and vascular development (BRI1, BRL1, BRL3, VH1, PXY, PXL1, PXL2)

procambium in the root. Our GFP analysis confirms expression within the vasculature. Our results, together with the publicly available data, indicate At5g49660 expression is restricted to vascular tissues, most likely phloem and procambium.

At5g49660 mutants display defects in vascular organization and phloem differentiation in inflorescence stems

Based on the expression of At5g49660 in the vasculature, we examined the morphology of the vasculature in plants carrying the S677P mutation, as well as the insertion mutation in At5g49660. Inflorescence stems from 6-week-old mutants and their corresponding wild-type accessions were hand-sectioned and stained with toluidine blue (TB), which binds lignin and stains the secondary cell walls of the xylem blue and the primary cell walls of the phloem and pith cells purple (Fig. 4a–f). In stems from both the missense and insertion mutants, aberrant blue staining was found within the phloem (Fig. 4b, d). Based on this mutant phenotype of xylem-like lignification of phloem we named

At5g49660 XIP1, with the missense mutation denoted as *xip1-1* and the insertion mutation as *xip1-2*. This staining of the phloem cells in *xip1* mutants was only observed at the base of the stem, within 2–3 cm from the base of the rosette. *xip1-1* plants transformed with the XIP1:GFP translational fusion have normal growth and also did not show aberrant blue staining of phloem cells when stem sections were stained with TB (Fig. 4e, f). Staining with phloroglucinol-HCl, which stains lignified cells red, gave similar results. Red-staining lignified cells were visible in the phloem region in *xip1-1* and *xip1-2* mutants, but absent in wild-type controls (Fig. 4g, h, i, j). Although the TB and phloroglucinol-HCl staining of phloem cells may be due to a partial transformation of phloem to xylem, the staining in the phloem is also consistent with the production of phloem fiber sclereids. Other than the intermixing of cells with xylem characteristics into the phloem in the *xip1-1* and *xip1-2* mutants, the vascular bundles appeared similar to wild type plants in morphology.

To identify the additional defects in vasculature identity in *xip1* mutants, hand-cut sections were further analyzed using aniline blue, which causes callose in the xylem to fluoresce blue and sieve plates in the phloem to fluoresce yellow under UV light (Fig. 4k–n). Aniline blue stained *xip1-1* and *xip1-2* sections showed blue fluorescence in the phloem region, confirming the presence of some cells with altered secondary walls in the phloem (Fig. 4l, n). Yellow fluorescing cells in the phloem of *xip1* mutants indicate that at least some of the cells in this region retain phloem identity, while other cells show aberrant lignification. In addition, in *xip1-1* mutants, phloem cells were located adjacent to xylem, in the region normally occupied by the procambium (8/12 plants) (insert in Fig. 4j). This phenotype, which is typical of *pxy* mutants, was less obvious in *xip1-2* plants (4/12 plants) and never seen in wild-type controls. The differences between the *xip1-1* allele and *xip1-2* allele could be attributed to accession differences.

The type of lignin deposited in the cell walls of xylem cells differs from the lignin found in the interfascicular region, the lignified tissue formed between xylem bundles in cambial growth. Interfascicular fibers stain red after treatment with Maule reagent due to the presence of syringyl type (s-type) lignin, and xylem cells appear brown due to a reduction or absence of s-type lignin. Hand-cut sections of wild-type and mutant inflorescence stems were stained with Maule reagent to determine the distribution of s-type lignin (Fig. 4o–r). Cells in the phloem region of *xip1-1* (12/12) and *xip1-2* (12/12) sections showed red staining similar to the stained regions of interfascicular fibers, indicating the presence of s-type lignin (Fig. 4p, r). Red stained phloem cells were never observed in wild-type sections ($n = 12$ each for Col-0 and Nos).

Fig. 3 XIP1 is expressed in the vasculature throughout plant development. **a** GUS staining in the mature embryo. **b** XIP1 expression in the vasculature of the inflorescence stem. Hand-cut sections show GUS staining in the vasculature and at the base (**c**, **d**) and apical region of the stem (**e**). **f**, **g** Vascular expression in veins of whole leaves and hand-cut cross sections. **h** XIP1 is expressed throughout the vasculature of petals and sepals. **i** XIP1 expression in hand-cut sections of petioles. **j** GUS staining in the hypocotyl. **k**, **l** XIP1 expression in the root vasculature based on analysis of GUS expression from a promoter fusion (**k**) and GFP expression from a translational fusion (**l**). *p* Phloem, *xy* xylem. *Scale bar* 50 μm
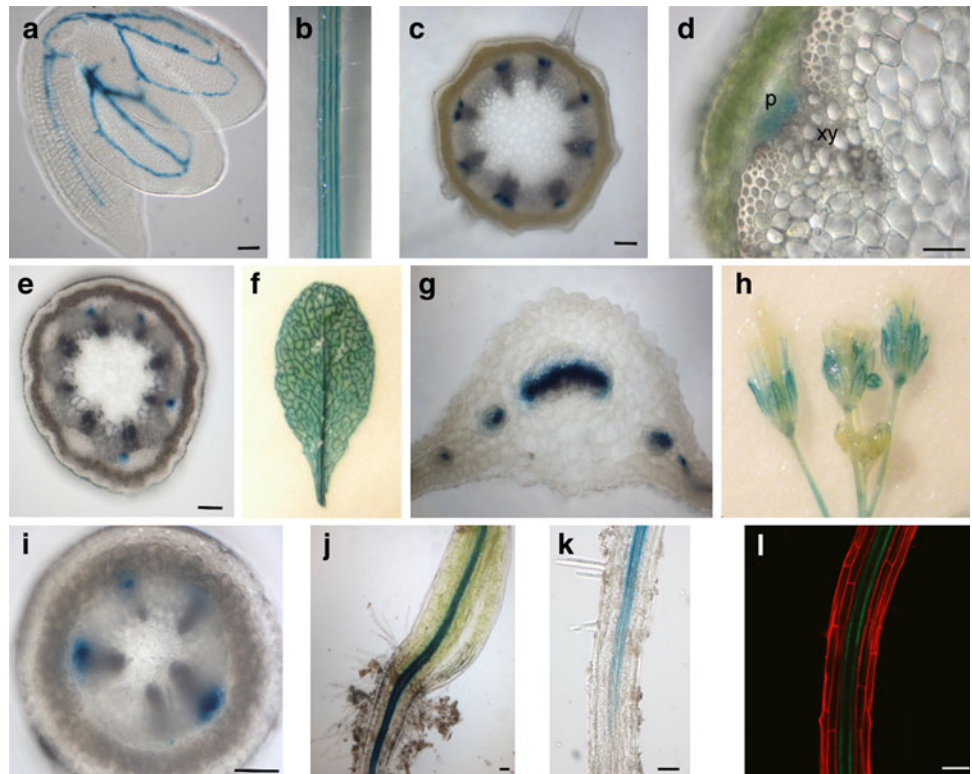
Longitudinal sections of *xip1* mutants show malformed vascular cells

Vascular cells need to be aligned with one another at their apical and basal ends to create conductive elements for transport of water, nutrients and small molecules. To determine whether *xip1* mutants have an altered arrangement of vascular cells that contributes to their growth defects, thin longitudinal sections of mutant and wild-type stems cut from the base were examined. The apical and basal boundaries of cells will be clearly visible if cells lie in the same optical plane and therefore constitute a continuous cell file, as can be seen in the pith cells in the sections from both wild-type and *xip1* plants (Fig. 5a–d). In sections from wild-type plants, vascular cells lie within the same optical plane and both apical and basal boundaries of the cells are visible (Fig. 5a, c). In contrast, *xip1* vascular cells have less visible apical and basal cell boundaries and instead have a "bottle-shaped" appearance, whereas the pith cells appear wild-type in the *xip1* sections (Fig. 5b, d). These data may indicate that vascular vessels show an alteration in the orientation and alignment of cells or the morphology of the vascular cells in *xip1* stems is disrupted.

We further examined the structure of the vasculature in whole-mount stems. After staining stems with propidium iodide, we were able to visualize xylem elements in apical stems (Przemeck et al. 1996). In wild-type stems, xylem elements were visualized as continuous vessels (Fig. 5e, g).

xip1 mutants showed discontinuous or misaligned xylem cells (Fig. 5f, h). Misalignment of xylem elements in the *xip1* mutants was visible in the apical portion of the stems, suggesting XIP1 is necessary for vascular development throughout the stem. Therefore, in addition to phloem specification defects, xylem vessel formation is also disrupted in *xip1* mutants.

Discussion

XIP1 is a regulator of vascular development

Coordinated cellular patterning and growth are necessary for proper formation of the vascular system in plants. In this study, we have identified a previously uncharacterized LRR RLK, XIP1, which is expressed mainly in the vasculature in *Arabidopsis*. We identified a mutant allele in XIP1 using TILLING and a transposon insertion that resulted in plants with several growth defects, including slower growth of the inflorescence stem and accumulation of anthocyanin in leaves. Further analysis showed defects in the development of the vasculature, specifically in phloem and xylem development. Using histochemical analyses, we showed that *xip1* phloem cells develop modified secondary walls resembling xylem or fiber cells. In addition, *xip1* phloem cells were sometimes adjacent to xylem cells, in the position of procambium cells, and the
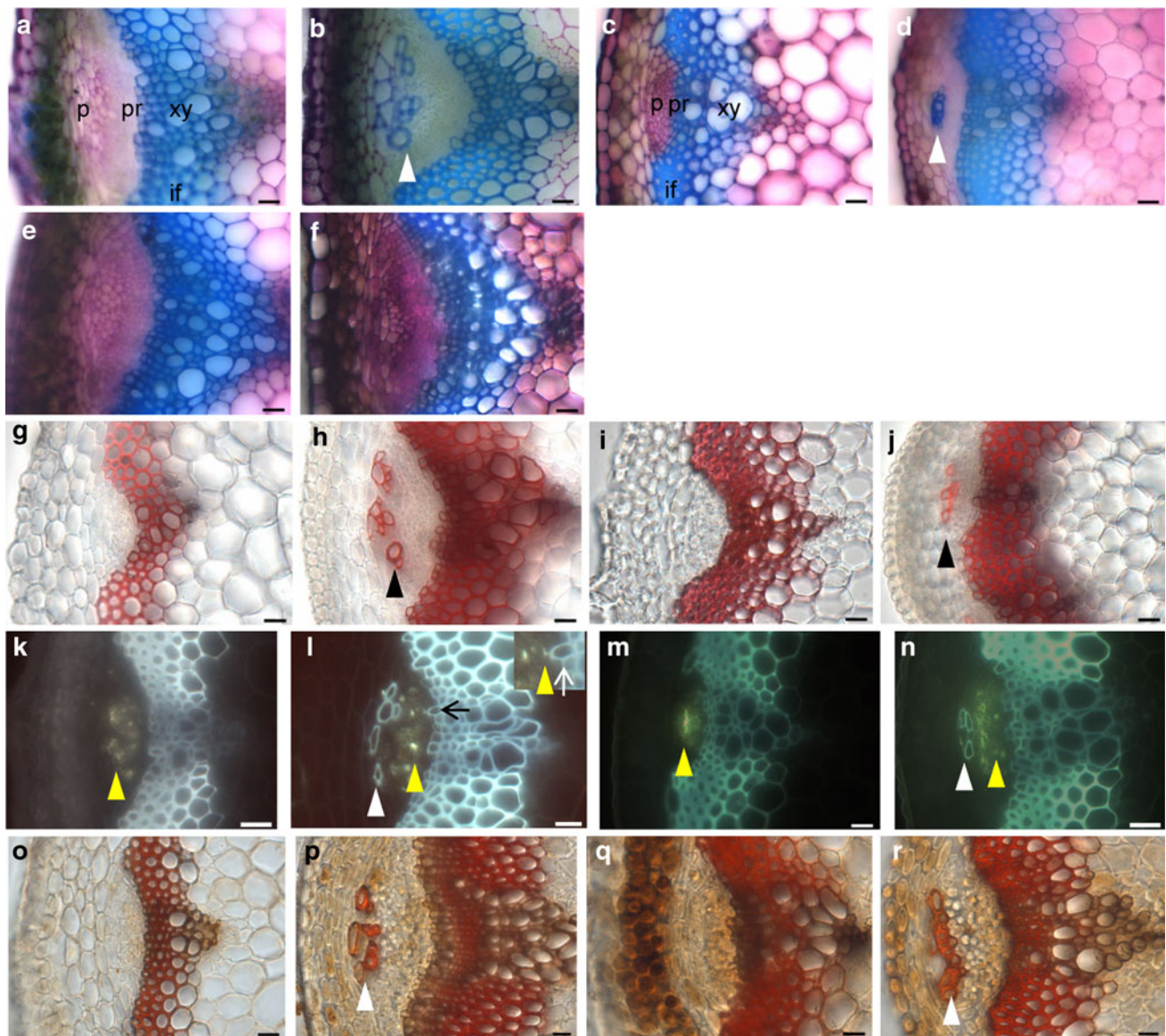
Fig. 4 Hand-cut cross sections of *xip1* inflorescence stems show aberrant xylem like cells within the phloem. Toluidine blue staining of 6-week-old inflorescence stems of Col-0 (**a**), Nos (**c**), *xip1-1* (**b**) and *xip1-2* (**d**). Lignin stains blue in xylem (xy) and interfascicular fibers (if) in wild-type and also within phloem (p) in *xip1-1* and *xip1-2* (*white arrow heads*). Toluidine blue staining of 6-week-old inflorescence stems of Col-0 (**e**) and *xip1-1* (**f**) plants transformed with the XIP1:GFP translational fusion. Phloroglucinol staining of Col-0 (**g**), *xip1-1* (**h**), Nos (**i**), and *xip1-2* (**j**) hand-cut sections indicating total lignin with ectopic lignin deposition seen in phloem (*black arrow heads*) of *xip1-1* and *xip1-2* sections (**h**, **j**). Aniline blue staining of wild-type Col-0 (**k**), Nos (**m**), *xip1-1* (**l**) and *xip1-2* (**n**) hand-cut sections of 6-week-old inflorescence stems. *Blue color* indicates callose deposition in xylem (*yellow arrow heads*) in wild-type Col-0 (**k**) and Nos (**m**) and xylem and phloem (*white arrow heads*) in *xip1-1* (**l**) and *xip1-2* (**n**). *Yellow fluorescent cells* indicate sieve elements in phloem cells with *yellow cells* adjacent and intermixed with xylem (*black arrow*) in *xip1-1* sections (**l**, inlay). Maule reagent staining of hand-cut sections shows staining of s-type lignin in interfascicular fibers in Col-0 (**o**) and Nos (**q**) and in both interfascicular fibers and the phloem region (*white arrow heads*) in *xip1-1* (**p**) and *xip1-2* (**r**). Xylem cells stain brown. *Scale bar* 50 μm

vessel elements do not appear to align in linear cell files or show abnormal morphology.

The *xip1-1* mutant allele is a missense mutation that results in a substitution of a serine to a phenylalanine in the kinase domain, which could eliminate an important phosphorylation site affecting the activity or function of XIP1. This serine residue shows some conservation in other related LRR RLKs including HAIKU2 (IKU2), involved in endosperm development, PXY-LIKE 2 (PXL2), related to and proposed to be redundant with PXY, and PEP1 RECEPTOR 1 and 2 (PEPR1/2), involved in defense response (Fig. 2) (Luo et al. 2005; Yamaguchi et al. 2006; Fisher and Turner 2007; Yamaguchi et al. 2010). The similar phenotypes seen in the insertion allele of XIP1,
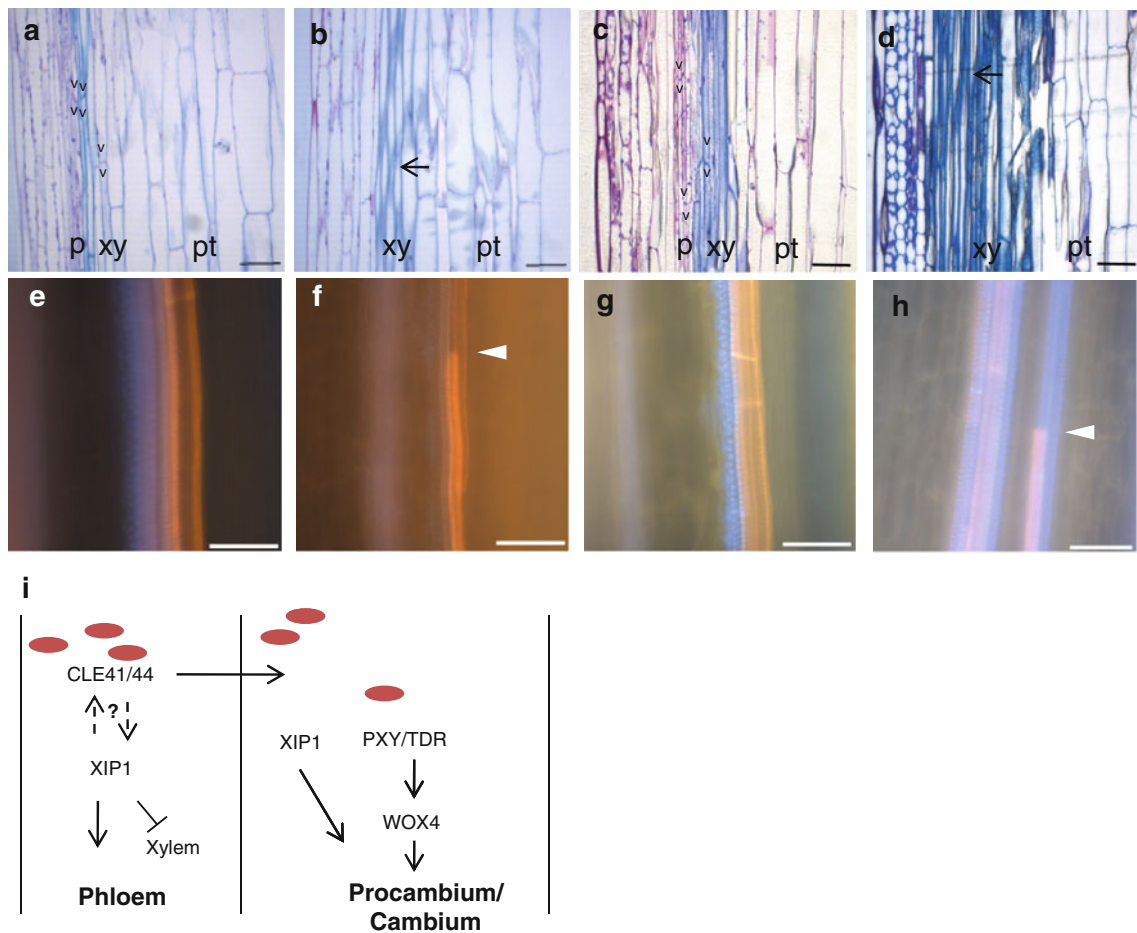
Fig. 5 Longitudinal sections of *xip1* inflorescence stems. Longitudinal sections of Col-0 (**a**), *xip1-1* (**b**), Nos (**c**) and *xip1-2* (**d**) 6-week-old inflorescence stems. Apical and basal end of xylem (xy) and pith (pt) cells can be seen in the plane of the section in wild type. Connected vessels (v) can be seen in both Col-0 and Nos sections. Apical and basal end of cells appear in focus only in pith cells in *xip1-1* (**b**) and *xip1-2* (**d**) sections and vascular cells the boundaries appear out of the plane of section (*arrows*). Cells with aberrant morphology can be seen in the xylem of *xip1-1* (**b**) and *xip1-2* (**d**). Whole-mount apical regions of stems stained with propidium iodide show visible xylem tracheary elements as fluorescent cells. Col-0 (**e**) and Nos (**g**) show continuous vessels compared to discontinuous elements (*white arrow heads*) seen in *xip1-1* (**f**) and *xip1-2* (**h**). **i** Model depicting likely locations and functions of XIP1 within the vascular tissues. CLE41/44 peptide originates from phloem cells and signals to PXY in the procambium to regulate WOX4, and to orient cell divisions and to maintain the fate of the procambium. XIP1 receives an as yet unknown signal, and prevents xylem or fiber formation and regulates vascular differentiation, which may have downstream consequences for phloem identity and CLE41/44 expression. **a–d** *Scale bar* 50 μm, **e–h** *scale bar* 20 μm

xip1-2, compared to *xip1-1* suggests both represent loss-of-function alleles. The slightly stronger *xip* phenotype observed with *xip1-1* mutant may be due to differences in the background accessions or due to altered activity of XIP1 in this mutant. However, *xip1-1* phenotypes are recessive, suggesting the differences are mostly likely due to accession differences.

We propose that the disrupted specification and organization of the vascular cells in *xip1* leads to less efficient vascular transport that impairs growth of inflorescence stems. The requirement for coordinated cell division and specification of vascular cells to maintain cell files would imply that disruption of these developmental patterns would lead to a disorganized vascular system. Indeed, several other examples of defects in vascular development result in plants with shorter inflorescent stems (Hanzawa et al. 2000; Pineau et al. 2005; Fisher and Turner 2007). In particular, *pxy* mutants, which show altered orientation of the divisions in the procambium, have reduced inflorescence stem height as well as the accumulation of anthocyanin in the cotyledons, similar to what we observe for *xip1* mutants (Fisher and Turner 2007). Defects in vessels, due to misaligned vascular cells or abnormal morphology, may form a vasculature that does not function as effectively in transport which may lead to shorter plants with more physiological stress, as indicated by the anthocyanin accumulation.

XIP1 and other receptor kinases in vascular development

Recent reports have described the LRR RLK PXY/TDR to be part of a signaling pathway required for maintaining procambium/cambium function, including promoting proliferation within the procambium and suppressing xylem cell differentiation (Hirakawa et al. 2010). In this pathway, the CLE41/44/TDIF peptide is secreted from phloem cells and interacts with PXY/TDR in the procambium/cambium (Fig. 5i). The CLE41/44/TDIF-PXY/TDR network induces the expression of WOX4, a WUS-like transcription factor, specifically in the procambium/cambium and promotes proliferation (Fig. 5f) (Ji et al. 2009; Hirakawa et al. 2010). The histochemical analyses of the xip1 mutants indicate the abnormal development of lignified phloem cells could be caused by either a phloem to xylem cell fate transformation, or due to abnormal differentiation due to cambium activity. Because xip1 mutants also develop a phloem intermixed with xylem phenotype similar to pxy mutants, the XIP1 name is appropriate, although it is still an open question as to whether there is a phloem to xylem transformation in xip1 mutants.

The appearance of phloem cells adjacent to xylem cells and the malformed alignment/morphology of cells in xip1 stems is similar to what is seen in pxy mutants, indicating that in xip1 mutants either (1) PXY signaling may be disrupted, perhaps by loss of CLE peptide signaling, thus affecting cambium activity and oriented cell divisions or (2) XIP1 may be involved in the regulation of cambium proliferation directly. Procambium activity/formation has been previously postulated to be regulated through the action of several KANADI genes (Eshed et al. 2001; Ilegems et al. 2010). These genes are predominantly expressed in the phloem and they are hypothesized to restrict procambium precursor cell formation through suppression of the auxin efflux carrier PIN1. In our model, XIP1 may be acting in a feedback mechanism through the CLE41/44/TDIF peptide-PXY-WOX4 pathway or through a separate pathway that regulates cambium activity and phloem cell differentiation (Fig. 5f).

A similar feedback pathway has been postulated for regulating meristem maintenance in the SAM. Although the effect on the WUS/WOX transcription factors is different, meristem maintenance of the SAM requires signaling from CLV3-CLV1/BAM1/2/CRN/CLV2 (CLE-LRR RLK interaction) to repress the expression of WUS. There is also a feedback mechanism that maintains this pathway. Our model, based on previous analysis of PXY/TDR suggests a CLE- LRR RLK module acts in a mechanistically similar way to maintain the meristem cells throughout the Arabidopsis vasculature. One extension of our model is that XIP1 could perceive signals from the procambium/cambium, to regulate phloem differentiation. A better understanding of how XIP1, PXY and PXL2 signaling pathways function independently or together to regulate the procambium/cambium and differentiation of phloem/xylem will contribute greatly to the mechanisms regulating vascular stem cell populations in plants.

Possible XIP1 function in secondary growth

The presence of the xip1 phenotype only at the base of the inflorescence stem suggests the defects may be attributed to abnormal secondary growth, a process regulated by the cambial meristem. The procambial meristem develops into the cambial meristem, which in turn regulates the formation of secondary xylem and phloem tissues. This secondary meristem is responsible for radial growth in adult plants. In Arabidopsis, cambium development appears restricted to the base of the inflorescence stem, hypocotyls and upper portion of the root. Our observation that defects are restricted to the base of the stem in xip1 plants suggests XIP1 may be important for secondary growth and development in stems. However, XIP1 is expressed in the vasculature throughout development, which suggests that XIP1 may play a redundant role in vascular development.

The abnormal phloem cell phenotype that we see in xip1 plants is reminiscent of the phenotype associated with AtHB8, a transcription factor involved in procambium/cambium development. Over-expression of AtHB8 is proposed to increase vascular cell differentiation and secondary growth. The staining of stem cross-sections from AtHB8 over-expressing plants with toluidine blue showed the presence of blue stained cells in the phloem, similar to xip1 mutants (Baima et al. 2001). The authors propose these cells as phloem fiber sclereids because of their thick secondary cell walls. Phloem fiber sclereids can originate from primary or secondary meristems such as the cambium (Lev-Yadun 1994). Ectopic fiber sclereid formation in the pith cells of wild type Arabidopsis due to repeated cutting of the stems (Lev-Yadun 1994) is likely a result of enhanced cambium activity. The staining pattern of s-type lignin in xip1 mutants is also consistent with a defect in phloem fiber sclereid formation in xip1 mutants. It is possible that XIP1 may function to perceive signals from the procambium/cambium to regulate the differentiation of phloem cells, or that XIP1 perceives a signal that restricts procambium/cambium activity. The presence of cells in the phloem with modified secondary cell walls raises the question if the procambium/cambium meristems are also "over-active" in xip1 plants. Indeed, mutants with overactive procambium and cambium, including over-expressing AtHB8 and high cambium activity (hca) mutants, show a significant decrease in plant height (Baima et al. 2001; Pineau et al. 2005).

The lignified secondary cell walls seen in the phloem of *xip1* mutants are similar to the phenotype of *pxy-like 1* (*pxl1*) double mutants with either *pxy* or *pxl2*, as described in Fischer and Turner (2007). It is not yet clear if XIP1 acts independently to repress ectopic lignification in the phloem, or acts together with PXY, PXL1 or PXL2 in the vasculature to regulate various aspects of procambium/cambium activity and vascular cell fate determination. Both *pxy* and *xip1* mutants also show defects in oriented cell divisions shown by disorganized cell files and phloem located near xylem cells, the *pxy* phenotype. Loss of either *pxy* or *xip1* results in reduced plant growth and this phenotype may be due to defects in cell division throughout the vasculature of the plant or to the disrupted transport system. These results indicate PXY and XIP1 may play a global role in the vasculature of all other organs as well. Continued analysis of these receptors and their interactions will provide further insight in the gene networks required for vascular development.

References

Agusti J, Lichtenberger R, Schwarz M, Nehlin L, Greb T (2011) Characterization of transcriptome remodeling during Cambium formation identifies MOL1 and RUL1 as opposing regulators of secondary growth. PLoS Genet 7(2):e1001312

Altamura MM, Possenti M, Matteucci A, Baima S, Ruberti I, Morelli G (2001) Development of the vascular system in the inflorescence stem of *Arabidopsis*. New Phytol 151(2):381–389

Baima S, Possenti M, Matteucci A, Wisman E, Altamura MM, Ruberti I, Morelli G (2001) The *Arabidopsis* ATHB-8 HD-Zip protein acts as a differentiation-promoting transcription factor of the vascular meristems. Plant Physiol 126(2):643–655. doi:10.1104/pp.126.2.643

Birnbaum K, Shasha DE, Wang JY, Jung JW, Lambert GM, Galbraith DW, Benfey PN (2003) A gene expression map of the *Arabidopsis* Root. Science 302(5652):1956–1960. doi:10.1126/science.1090022

Bonke M, Thitamadee S, Mahonen AP, Hauser M-T, Helariutta Y (2003) APL regulates vascular tissue identity in *Arabidopsis*. Nature 426(6963):181–186

Brady SM, Orlando DA, Lee J-Y, Wang JY, Koch J, Dinneny JR, Mace D, Ohler U, Benfey PN (2007) A high-resolution root spatiotemporal map reveals dominant expression patterns. Science 318(5851):801–806. doi:10.1126/science.1146265

Brand U, Grunewald M, Hobe M, Simon R (2002) Regulation of CLV3 expression by two homeobox genes in *Arabidopsis*. Plant Physiol 129(2):565–575. doi:10.1104/pp.001867

Clark SE, Running MP, Meyerowitz EM (1993) CLAVATA1, a regulator of meristem and flower development in *Arabidopsis*. Development 119(2):397–418

Clark SE, Williams RW, Meyerowitz EM (1997) The CLAVAT-A1Gene encodes a putative receptor kinase that controls shoot and floral meristem size in *Arabidopsis*. Cell 89(4):575–585

Clough SJ, Bent AF (1998) Floral dip: a simplified method for *Agrobacterium*-mediated transformation of *Arabidopsis thaliana*. Plant J 16(6):735–743

Donner TJ, Sherr I, Scarpella E (2009) Regulation of preprocambial cell state acquisition by auxin signaling in *Arabidopsis* leaves. Development 136(19):3235–3246. doi:10.1242/dev.037028

Eshed Y, Baum SF, Perea JV, Bowman JL (2001) Establishment of polarity in lateral organs of plants. Curr Biol 11(16):1251–1260

Fisher K, Turner S (2007) PXY, a receptor-like kinase essential for maintaining polarity during plant vascular-tissue development. Curr Biol 17(12):1061–1066

Galweiler L, Guan C, Muller A, Wisman E, Mendgen K, Yephremov A, Palme K (1998) Regulation of polar auxin transport by AtPIN1 in *Arabidopsis* vascular tissue. Science 282(5397):2226–2230. doi:10.1126/science.282.5397.2226

Gou X, He K, Yang H, Yuan T, Lin H, Clouse S, Li J (2010) Genome-wide cloning and sequence analysis of leucine-rich repeat receptor-like protein kinase genes in *Arabidopsis thaliana*. BMC Genomics 11(1):19

Guo D, Chen F, Inoue K, Blount JW, Dixon RA (2001) Downregulation of caffeic acid 3-O-methyltransferase and caffeoyl coa 3-o-methyltransferase in transgenic alfalfa: impacts on lignin structure and implications for the biosynthesis of G and S lignin. Plant Cell Online 13(1):73–88. doi:10.1105/tpc.13.1.73

Hanzawa Y, Takahashi T, Michael AJ, Burtin D, Long D, Pineiro M, Coupland G, Komeda Y (2000) ACAULIS5, an *Arabidopsis* gene required for stem elongation, encodes a spermine synthase. EMBO J 19(16):4248–4256

Hirakawa Y, Shinohara H, Kondo Y, Inoue A, Nakanomyo I, Ogawa M, Sawa S, Ohashi-Ito K, Matsubayashi Y, Fukuda H (2008) Non-cell-autonomous control of vascular stem cell fate by a CLE peptide/receptor system. Proc Natl Acad Sci 105(39):15208–15213. doi:10.1073/pnas.0808444105

Hirakawa Y, Kondo Y, Fukuda H (2010) TDIF peptide signaling regulates vascular stem cell proliferation via the WOX4 homeobox gene in *Arabidopsis*. Plant Cell Online 22(8):2618–2629. doi:10.1105/tpc.110.076083

Ilegems M, Douet V, Meylan-Bettex M, Uyttewaal M, Brand L, Bowman JL, Stieger PA (2010) Interplay of auxin, KANADI and Class III HD-ZIP transcription factors in vascular tissue formation. Development 137(6):975–984. doi:10.1242/dev.047662

Ji J, Strable J, Shimizu R, Koenig D, Sinha N, Scanlon MJ (2009) WOX4 promotes procambial development. Plant Physiol 152(3):1346–1356. doi:10.1104/pp.109.149641

Kang J, Dengler N (2002) Cell cycling frequency and expression of the homeobox gene ATHB-8 during leaf vein development in *Arabidopsis*. Planta 216(2):212–219

Kubo M, Udagawa M, Nishikubo N, Horiguchi G, Yamaguchi M, Ito J, Mimura T, Fukuda H, Demura T (2005) Transcription switches for protoxylem and metaxylem vessel formation. Genes Dev 19(16):1855–1860. doi:10.1101/gad.1331305

Lev-Yadun S (1994) Induction of sclereid differentiation in the pith of *Arabidopsis thaliana* (L.) Heynh. J Exp Bot 45(12):1845–1849. doi:10.1093/jxb/45.12.1845

Luo M, Dennis ES, Berger F, Peacock WJ, Chaudhury A (2005) MINISEED3 (MINI3), a WRKY family gene, and HAIKU2 (IKU2), a leucine-rich repeat (LRR) KINASE gene, are regulators of seed size in *Arabidopsis*. Proc Natl Acad Sci 102(48):17531–17536. doi:10.1073/pnas.0508418102

Lux A, Morita S, Abe JUN, Ito K (2005) An improved method for clearing and staining free-hand sections and whole-mount samples. Ann Bot 96(6):989–996. doi:10.1093/aob/mci266

Pineau C, Freydier A, Ranocha P, Jauneau A, Turner S, Lemonnier G, Renou J-P, Tarkowski P, Sandberg G, Jouanin L, Sundberg B, Boudet A-M, Goffner D, Pichon M (2005) hca: an *Arabidopsis* mutant exhibiting unusual cambial activity and altered vascular patterning. Plant J 44(2):271–289

Przemeck GKH, Mattsson J, Hardtke CS, Sung ZR, Berleth T (1996) Studies on the role of the *Arabidopsis* gene MONOPTEROS in vascular development and plant cell axialization. Planta 200(2):229–237

Sarkar AK, Luijten M, Miyashima S, Lenhard M, Hashimoto T, Nakajima K, Scheres B, Heidstra R, Laux T (2007) Conserved factors regulate signalling in *Arabidopsis thaliana* shoot and root stem cell organizers. Nature 446(7137):811–814

Scheres B, Di Laurenzio L, Willemsen V, Hauser MT, Janmaat K, Weisbeek P, Benfey PN (1995) Mutations affecting the radial organisation of the *Arabidopsis* root display specific defects throughout the embryonic axis. Development 121(1):53–62

Schoof H, Lenhard M, Haecker A, Mayer KFX, Jürgens G, Laux T (2000) The stem cell population of *Arabidopsis* shoot meristems is maintained by a regulatory loop between the CLAVATA and WUSCHEL genes. Cell 100(6):635–644

Shiu S-H, Bleecker AB (2001) Receptor-like kinases from *Arabidopsis* form a monophyletic gene family related to animal receptor kinases. Proc Natl Acad Sci 98(19):10763–10768. doi:10.1073/pnas.181141598

Stahl Y, Simon R (2010) Plant primary meristems: shared functions and regulatory mechanisms. Curr Opin Plant Biol 13(1):53–58

Stahl Y, Wink RH, Ingram GC, Simon R (2009) A signaling module controlling the stem cell niche in *Arabidopsis* root meristems. Curr Biol 19(11):909–914

Till BJ, Reynolds SH, Greene EA, Codomo CA, Enns LC, Johnson JE, Burtner C, Odden AR, Young K, Taylor NE, Henikoff JG, Comai L, Henikoff S (2003) Large-scale discovery of induced point mutations with high-throughput TILLING. Genome Res 13(3):524–530. doi:10.1101/gr.977903

Yamaguchi Y, Pearce G, Ryan CA (2006) The cell surface leucine-rich repeat receptor for AtPep1, an endogenous peptide elicitor in *Arabidopsis*, is functional in transgenic tobacco cells. Proc Natl Acad Sci 103(26):10104–10109. doi:10.1073/pnas.0603729103

Yamaguchi Y, Huffaker A, Bryan AC, Tax FE, Ryan CA (2010) PEPR2 is a second receptor for the pep1 and pep2 peptides and contributes to defense responses in *Arabidopsis*. Plant Cell Online 22(2):508–522. doi:10.1105/tpc.109.068874

Ye Z-H (2002) Vascular tissue differentiation and pattern formation in plants. Annual Review Plant Biol 53(1):183–202. doi:10.1146/annurev.arplant.53.100301.135245